



A hybrid metaheuristic assisted collateral fractional-order controller for three-phase solar PV, BESS, and wind- integrated UPQC

Shravan Kumar Yadav¹ · Krishna Bihari Yadav¹

Accepted: 22 November 2023 / Published online: 30 January 2024

© The Author(s), under exclusive licence to Springer-Verlag GmbH Germany, part of Springer Nature 2024

Abstract

Due to the environment's instability, to reduce inconsistent power supply it is preferable to connect two or more RES in a grid. Harmonics and other power quality issues are introduced into the distribution grid as a result of integrating these Hybrid Renewable Energy Storage (HRES) with nonlinear loads, which is a significant concern for the utility and the consumers, respectively. With the use of the Unified Power Quality Conditioner (UPQC), power quality problems such as voltage interruptions, actual power, and reactive power can be reduced. For optimal operation of the series and shunt compensator of UPQC, the outputs of the converters are controlled by PWM signals, which are optimally tuned by controllers implemented with updated algorithms. An optimized Hybrid metaheuristic-assisted collateral controller comprising of fractional-order proportional integral derivative (FOPID) controller cum (proportional integral (PI) controller for the enhancement of the Three-Phase HRES system-based Distribution Grid integrated with UPQC is developed in this paper. The UPQC reduces the harmonics that non-linear loads feed into the power supply and power quality concerns. The DC link voltage regulation and controller optimization are achieved with the optimal tuning of gain parameters, fractional orders and weight parameters using a hybrid Metaheuristic Algorithm named Amplified Slime Mould with WildeBeest Herd Optimization (ASM-WHO) Algorithm. The proposed system is developed in MATLAB Simulink to compare the effectiveness of compensation for voltage sags and surges and total harmonic distortion (THD) to more traditional approaches, UPQC with PI controller, FOPID-PI controller, FOPID-PI with Chicken Swarm Optimization (CSO), SOA, SMA, and WHO optimization. The settling time for the proposed FOPID-PI controller with ASM –WHO is 147.27 s, which is 1.7%, 13.78%, 1.338% and 13.66% better than the controller without optimization, the proposed collateral controller method with either SOA or CSO or SMA, WHO optimization and PI controller respectively.

Keywords UPQC · FOPID controller · PI controller · Shunt and series APF compensator

1 Introduction

Electricity has become a more indispensable form of energy that provides a highly adaptable human life. As the demand for electricity rises along with population growth and technological advancement, the conventional energy crisis increases. Hence, RES is used widely in power generation and distribution with global environmental and economic concerns (Qazi et al. 2019). Due to the

unstable nature of the environment, connecting two or more RES in a grid is preferred for the reduction of intermittent power supply (Carrasco et al. June 2006). Integration of these HRES with nonlinear loads introduces harmonics and other power quality problems in the distribution grid, which is a major issue for the utility and the consumers respectively (Latha et al. September 2011). Correcting the problems for reliable power transmission and supply is necessary to guarantee the quality of the electricity in the distribution system. The power quality issues, such as voltage interruptions, real power, and reactive power can be mitigated with the usage of Unified UPQC (Sivakumar et al. 2019) (Gowrishankar and Ramasamy 2020).

✉ Shravan Kumar Yadav
shravankumaryadav781@gmail.com

¹ Department of Electrical Engineering, National Institute of Technology, Jamshedpur, Jharkhand, India

The outputs of the converters are controlled by PWM signals, which are ideally tuned by controllers designed with updated algorithms, for the best performance of the series and shunt compensator of UPQC. The P&O algorithm implemented by MPPT was used to optimize the PI Controller in the PV–UPQC system (Samal and Hota 2017). Atom Search Optimization (ASO) Algorithm-based FOPID controller was used for the control of UPQC in the PV-Wind-BESS System (Goud and Loveswara Rao 2021). GSA algorithm for automatic tuning of PI controller parameters was used as the optimization control of UPQC in the distribution grid (Alam and Arya 2020). As a result, for tuning the gain parameter optimally more efficient system needs to be introduced (Privacy-preserving malware detection in Android-based IoT devices through federated Markov chains 2023; D’Angelo et al. 2023).

In this proposed method, Solar PV and Wind-based power generation systems are connected along with the BESS to reduce the intermittent supply in the distribution system. A novel control strategy is adopted to govern the shunt compensator of UPQC in the distribution grid integrated with interconnected RES by introducing a Collateral controller. It is a parallel connection of the FOPID controller and PI controller whose gains are optimally tuned by an innovative algorithm and summed up for effective power quality corrections. The weights and gain parameters are optimally tuned by the ASM-WHO Algorithm.

2 Objectives

To design and develop amplified slime mould with wildebeest herd optimization algorithm focuses on controller development for the optimal current and voltage compensation in UPQC compensators.

The following are this work’s main contributions:

- Introduces a collateral control model of FOPID controller shunted with PI Controller.
- Introduces a novel algorithm by updating the Wildebeest Herd Optimization algorithm with SMA.
- The optimal solution of WHO is given as an input to Slime Mould Algorithm, in which the best solution is attained for tuning the gain parameters and weight parameters.
- The DC link voltage regulation and controller optimization are attained with the optimal tuning of gain parameters, such as k_p, k_i, k_d fractional orders (λ, μ) and weight parameters (w_1, w_2) using a hybrid Metaheuristic Algorithm named Amplified Slime Mould with WildeBeest Herd Optimization (ASM-WHO) Algorithm.

The following is how this paper is organised: the current approaches are briefly reviewed in Sect. 2. The system setup of the HRES-integrated Distribution Grid with UPQC is described in Sect. 3. The developed ASM-WHO Algorithm for the optimization of FOPID and PI controller settings is described in Sect. 4. The outcomes of the implemented system are explained in Sect. 5, and Sect. 6 concludes with the article summary.

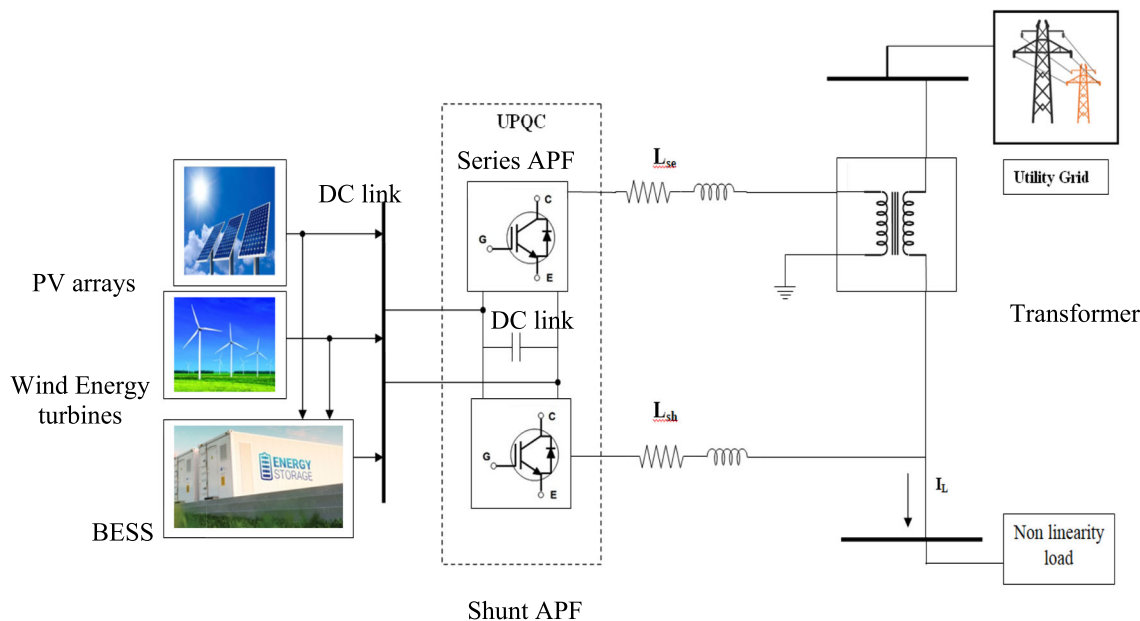


Fig.1 Diagrammatic representation of HRES—utility grid system integrated with UPQC

Fig. 2 Architecture of series controller

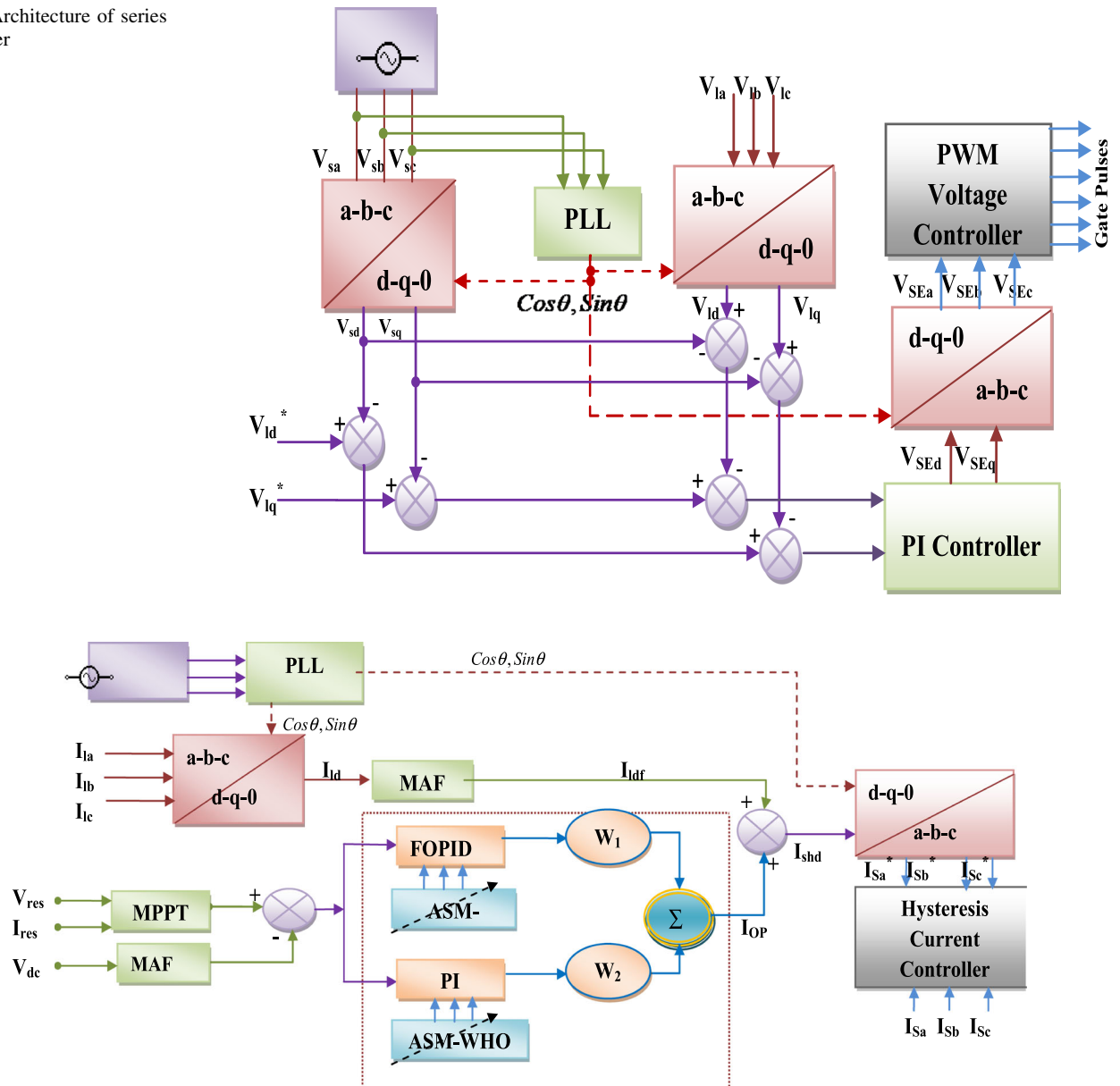


Fig. 3 Diagrammatic representation of Shunt Controller

3 Literature review

In 2020, Muhammad Murtadha Othman et al. (Mansor et al. 2020) developed a hybrid PV-BESS system with UPQC. An STF with a Unit vector Integration approach is implemented for phase synchronization of the Shunt Active Power Filter (APF) and Series APF and to address the unbalanced voltage and power quality problems by increasing the overall efficiency.

In 2020, R. Pavan Kumar Naidu and S. Meikandasivam (Naidu et al. 2020) developed FACTS-based Distributed Power Flow Controller (DPFC) Controller comprising a shunt and series compensator. It is also integrated with a

FOPID controller to solve the PQ issues that arise in the grid due to the connected hybrid source. It improves the voltage transition and voltage compensation with reduced oscillation.

In 2020, Tao jin et al. (Jin et al. 2020) established an efficient control approach for the UPQC-assisted dq0 detection technique, which eliminates PQ problems in power distribution. In the technique created an SVPWM algorithm with a fundamental and harmonic detection mechanism, which enhances PQ and results in superior tracking voltage performance.

In 2020, Ch. Sivakumar and Mallesham (Kumar and Mallesham 2020) developed a revolutionary design that

integrates RES, such as fuel cells and wind turbines with a squirrel cage induction motor to reduce greenhouse gas emissions. Also discussed is an Artificial Neural Network (ANN) controller-based UPQC that can tolerate voltage variations while enhancing PQ.

In 2020, V Nanthagopal et al. (Nanthagopal, Dr.S. Chitra. 2020) designed a unique technique for studying the solar integrated UPQC, which combines a shunt and series compensator with a shared DC-link, under current and voltage distortion. It enhances the system's stability and reduces voltage disturbances.

In 2021, Ch. Phani Kumar et al. (2021) described the importance of PQ improvement in an integrated hybrid grid energy system with UPQC. It uses discrete three-phase active power converters in series and shunt. The PSCAD simulation platform is used to simulate and analyse the system while a fuzzy logic controller performs the optimal tuning of UPQC. The system enhances PQ and provides effective harmonic reduction within the permissible level.

In 2021, Ch. Rami Reddy et al. (2021) designed a UPQC with an ASO Algorithm for the mitigation of PQ issues in the HRES system. The addition of an ASO-based FOPID controller improves UPQC performance. THD and PQ issues at two modes (Power injection > 0 and Power Injection < 0) are analyzed. It also retains the system's stability and durability.

In 2022, Tongfei Lei et al. (2022) dealt with the harmonics and voltage/current variations generated in the distributed generation system combined with UPQC. Since FFCL is dedicated to providing current series converter references, Wind-PV-UPQC is based on a dual compensation technique with the parallel converter and series converter. It achieves quick power balance and enhances the transition level of DC bus voltage and converter current.

In 2022, Mahdi (2022) have utilized UPQC with a sensitive load that is connected to a grid power system. Using pulse-width modulation and hysteresis as switching mechanisms, the UPQC will function under various disturbances such as phase-to-ground fault, non-linear load on the grid side, and non-linear load in parallel with the sensitive load. The two pulsing-generating systems are compared using simulation results from MATLAB/Simulink, which demonstrate that electrical power is constantly provided to the load in all disturbances with THD less than 5% for voltage and 4.5% for current.

In 2023, Thangella (2023) have described a control strategy for UPQC that combines the BESS (UPVBSS) and PV system. Introduced artificial neural network controller (ANNC) for UPQC series and MPPT for PV systems, shunting active filters to reduce THD, power factor, and overall it increases the power supply voltage to remove changes and maintain a constant DC-link voltage with

short settle point. Through the use of multiple test cases with different source and load characteristics, this study examines the performance of UPVBSS. The waveforms, power quality enhancement, total harmonic distortion (THD), and power factor all show good performance.

A self-tuning filter with a Unit vector Integration technique is implemented for phase synchronization of Shunt APF and Series APF in UPQC (Mansor et al. 2020). This enables the operation of distorted and imbalanced grid voltage circumstances. It overcomes the limitations of the DC capacitor system as it is connected with a BESS. In addition, it overcomes the disadvantages of the PLL filter by reducing THD and phase differences between the source voltage and current. However, it requires consideration of environment-dependent features due to unreliable renewable energy. A novel FACTS-based DPFC that integrates a coordinated PQ theory with the FOPID controller was introduced in Naidu et al. (2020). This reduces the ripples and provides a preferable voltage transition profile in the grid-connected hybrid system. However the switching frequency control must be added in addition to the hysteresis controller. An efficient UPQC control scheme based on the dq0 detection method and improved SVPWM technique was implemented in Jin et al. (2020). However, concern must be taken for the three-level SVPWM. The power quality optimization of PEMFC Wind energy systems was built by an ANN-based UPQC with an FFBL algorithm (Kumar and Mallesham 2020). The system handles voltage fluctuation and reduces PQ issues. However, needs consideration, especially in a weak grid system. A DVR with a PI controller was used as a series compensator in PV-UPQC (Nanthagopal et al. 2020). It increases the system's stability and reduces voltage disturbance. However, unwanted PQ disturbances may cause voltage collapse. HRES implemented with UPQC uses PLL-based FLC control (Phani et al. 2021). It improves system stability and lessens voltage fluctuations. Voltage breakdown, however, may result from unintended PQ disturbances. In UPQC connected with HRES, an ASO-based FOPID controller is utilised (Reddy et al. 2021). It offers efficient PQ issue mitigation while maintaining the system's stability and dependability. However, the harmonic reduction in voltage source and active power filtering procedure is not taken into account. A PV-wind UPQC uses FFCL for optimal control of harmonic distortions. It can achieve quick power balance and enhance the transition level of DC bus voltage and converter current. However, Only 3 out of 16 conditions are considered for the neutral point clamped inverter with transistors as others may induce a DC link short circuit. The FOPID controller outperforms all others in terms of voltage transition, compensation, and harmonic reduction.

4 Hybrid energy system configuration with UPQC integration

To overcome the aforementioned issues, the researchers innovate effective hybrid metaheuristic-assisted collateral fractional-order controller for three-phase solar PV, BESS, and wind-integrated UPQC. The implementation of HRES combining the BESS, PV array, and wind power generation system ensures continuous power production and distribution stability. The shunt compensator protects the load by regulating the current harmonics in the grid together with the maximum power extraction from the HRES, while the series compensator of UPQC lowers the voltage harmonics in the grid. By optimally tuning the gain parameters using a hybrid ASM-WHO algorithm the regulation in DC link voltage and controller optimization are attained.

4.1 Overview of system configuration

In the suggested system model, the power distribution system to nonlinear loads that is integrated with UPQC is shown diagrammatically in Fig. 1. The power source in this proposed model includes wind energy turbines, PV arrays, and BESS. PV arrays and wind turbines supply electric energy based on the availability of sunlight and wind respectively. Due to the controvert nature of the environmental climatic condition intermittent curbs may occur. For the incessant supply of electricity, a BESS is included. The BESS system supplies the unsatisfied amount of energy required for the load in addition to the simultaneous storage of energy. Moreover, the BESS can also act as a standalone power source to supply the total load demand when there is no alternative source (Nehrir et al. 2011).

Harmonics may be introduced to the grid by the connectivity of RES and the addition of nonlinear loads, which causes problems with power quality such as voltage sag, swell, and harmonic distortions. The widely used advanced power conditioner UPQC mitigates power quality problems (Khadkikar 2011). The distortion-free balanced load terminal voltage is maintained with the insertion of voltage by the series component of the UPQC, while the current in the bus is maintained to be sinusoidal with the insertion of current using the shunt component of the UPQC (Alam and Arya 2020). The voltage fluctuation between the shunt and series APF is controlled by a DC-link capacitor. The UPQC control heavily relies on reference signal generation (Singh et al. 2016). In consequence, a double harmonic component exists in the axis current during unbalancing load conditions which is filtered using the MAF (Singh et al. 2014). The grid synchronization is achieved by PLL.

4.2 Control of UPQC

To maintain a unity power factor, the load voltage and current are regulated by the series and shunt compensators. A shunt compensator is used to reduce harmonics and compensate for reactive power, and a series compensator shields the load from grid-side PQ problems. Moreover, the shunt compensator extracts more power from RES. The optimal power conditioning is achieved with optimal control of PWM Signals. The architecture of the series controller in UPQC is shown in Fig. 2.

The PLL extracts a fundamental PCC voltage component to generate a reference axis in dq0 with its phase and frequency information (Javadi et al. 2016). To generate appropriate reference signals, PI controllers exploit the discrepancy between the reference and actual series compensator voltages. To create adequate gate pulses of the series controller, these signals are translated to the a–b–c domain and fed via a PWM voltage controller (Sadigh and Smedley 2012). The architecture of the shunt controller is shown in Fig. 3.

The equivalent source current component is extracted from the power output of the RES interconnected bus and the voltage source component (Devassy and Singh 2017). The MPPT with INC algorithm is used to extract maximum power from the RES and the reference source voltage is compared with filtered dc-link capacitor voltage to draw a loss current using the optimal controller (Subudhi and Pradhan 2012). The shunt compensator optimization is performed using the proposed optimal controller to obtain a distortion-less load current at the DC-link reference voltage. Thus, the optimized current signals, such as I_{ldf} and I_{OP} gets concatenated to obtain,

$$I_{SHd}^* = I_{ldf} + I_{OP} \quad (1)$$

Thus, the procured current signal with an a–b–c reference frame is used to generate a gating pulse for the shunt compensator via the hysteresis current controller.

4.3 Proposed optimal controller

The shunt compensator controller employs an optimal collateral controller of a FOPID and a PI Controller optimized by a hybrid metaheuristic algorithm that blends the concepts of both WHO and SMA algorithms. These controllers are widely applied in industrial control systems that use a closed-loop DC-link capacitor voltage regulation method.

4.3.1 FOPID Controller

The FOPID controller is the more advanced version of the PID controller with fractional calculus that offers more

Table 1 Algorithm parameters

Algorithm	Parameters and values
CSO	G = 10 r = 0.15 h = 0.7 m = 0.5
SOA	b = 1
SMA	z = 0.03
WHO	n_s = 3 n_e = 3 = 0.15 local_move = [0.9, 0.3] global_move = [0.2, 0.8] p_hi = 0.9 delta Δ = [2.0, 2.0]
AO	Alpha α = 0.1 delta Δ=0.1 u = .0265 r0 = 10 omega ω= .005
HBA	beta β = 6 C = 2 N = 30
ASM-WHO	n_s = 3 η = 0.15 z = 0.03

tuning flexibility, durability, and frequency responsiveness (Jumani et al. 2020). The differential equation of the FOPID in time domain form is given by.

$$c_1(t) = K_p \left(e(t) + \frac{1}{T_i} D^{-\lambda} e(t) + T_d D^{\mu} e(t) \right) \quad (2)$$

where λ and μ are the fractional orders in which $\lambda = \mu = 1$. $e(t)$ represents the deviation between the values measured and set-point, k_p indicates the proportional gain, T_i and $s T_d$ are the integral and derivative time constants respectively and D is the fractional operator.

4.3.2 PI Controller

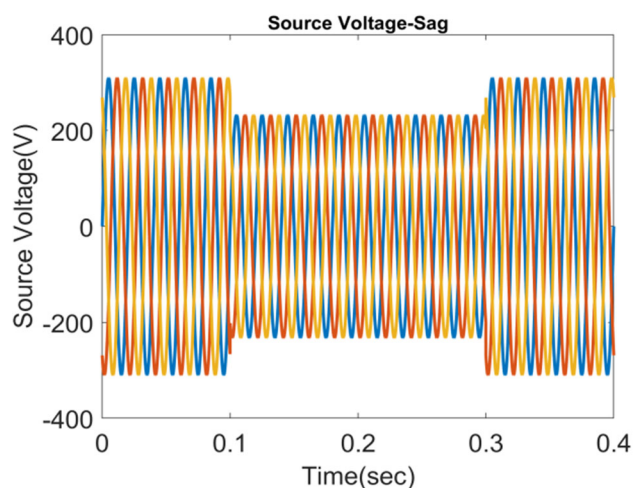
PI controller algorithm includes Proportional and Integral factors. The current error is determined by the proportional value, whereas the aggregate errors are determined by the integral value. The output of the PI controller may be expressed as

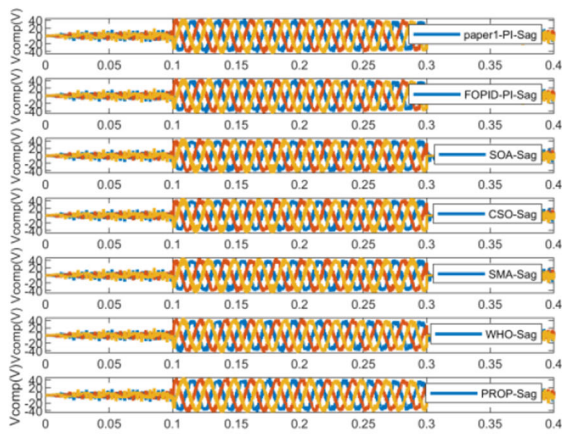
$$c_2(t) = K_p e(t) + K_i \int e(t) dt \quad (3)$$

where K_p and K_i represent the proportional gain and integral gain, respectively. The voltage error value e is provided to the FOPID-PI collateral controller. The optimal collateral controller output is fed into the shunt inverter's current control system, which draws the needed amount of active power from the grid to sustain the DC link voltage (O'Dwyer 2000).

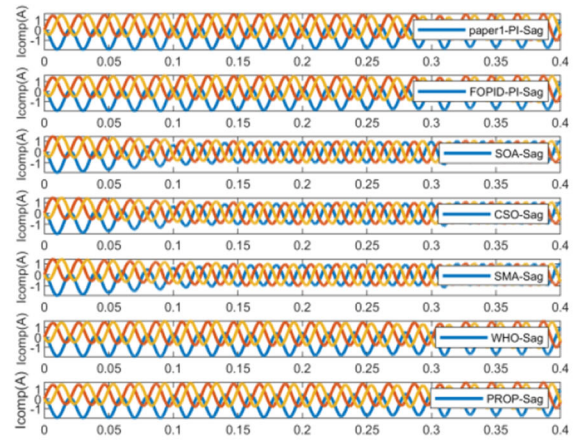
In the proposed work, the gain parameters, such as K_p and K_i of the PI controller, K_p, K_i, K_d , and fractional-order parameters, such as λ and μ of the FOPID controller, and the weight parameters including w_1 and w_2 are optimally tuned, which significantly influence the DC voltage regulation. The DC-link capacitor requires real power proportional to the deviated voltage between the actual and reference voltage values to retain capacitor voltage within its reference value.

DC-bus voltage regulation is dominant when gain parameters (K_p, K_i, K_d) are large, and steady-state dc-bus voltage error is minimal. When the gain parameters are small, however, the real power imbalance has no impact on transient performance. As a result, accurate selection is essential to meet control performance and sustain the capacitor's power requirements. In the first approach, the values (K_p, K_i, K_d) are selected at random. The following conditions must be considered while selecting K_p and K_i : a high value of K_p leads to control system instability and low K_p increases in the response time. The steady-state inaccuracy in the voltage control system is corrected by the integral gain of the controller. The UPQC efficiency under dynamic power system conditions can be achieved by fast DC link voltage control along with the maintenance of capacitor voltage with the shortest delay time and reduced overshoot.

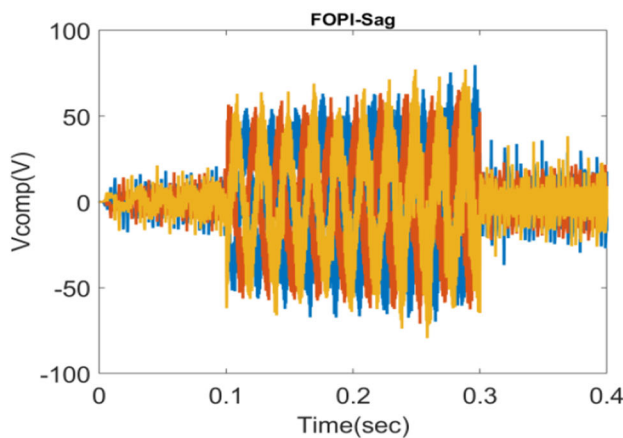
**Fig. 4** Source voltage waveform without UPQC



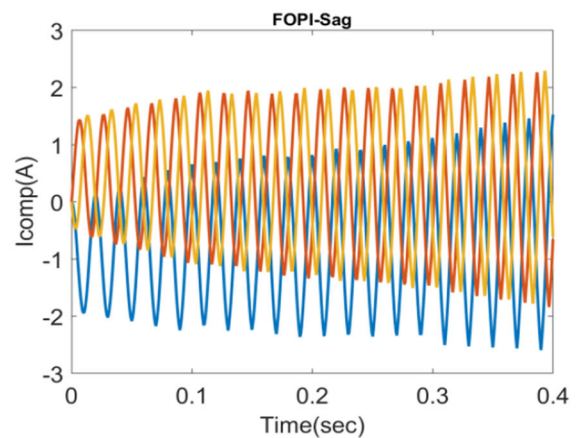
(a) Voltage Compensation waveform at sag (FOPID)



(b) Current Compensation waveform at sag (FOPID)

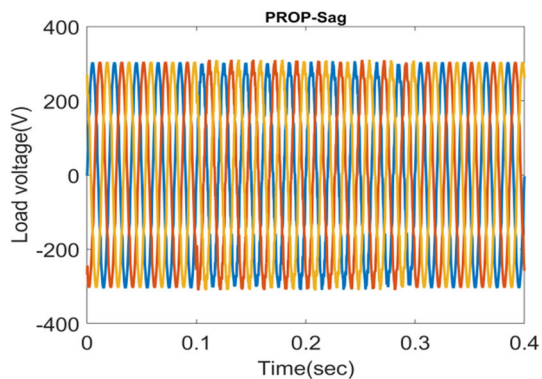


(c) Voltage Compensation waveform at sag (FOPI)

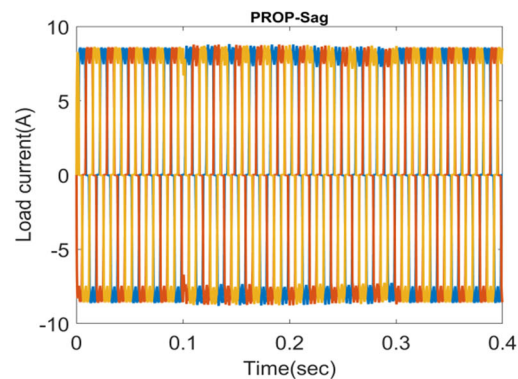


(d) Current Compensation waveform at sag (FOPI)

Fig. 5 Compensation of voltage and current waveforms at sag condition (a) Voltage for FOPID, (b) Current for FOPID, (c) Voltage for FOPI and (d) Current for FOPI



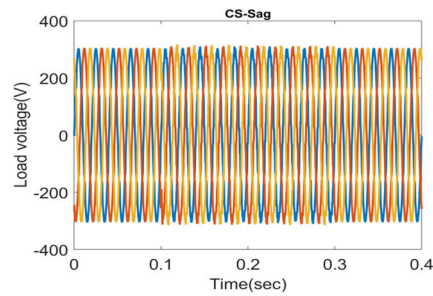
(a) Compensated load voltage waveform with proposed optimized controller



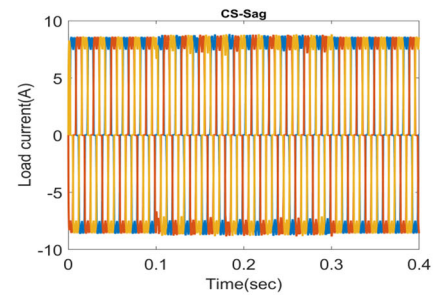
(b) Compensated load current waveform with proposed optimized controller

Fig. 6 Case 1—Compensated Load voltage and current waveform for the suggested approach under Sag condition

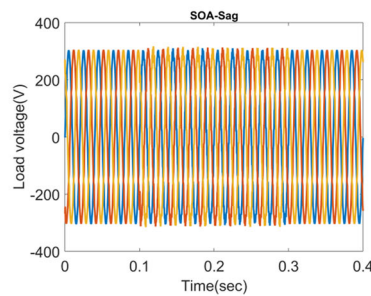
Fig. 7 Case 2—Comparison of Compensated Load voltage and current waveform of the suggested approach over the extant methods under Sag condition



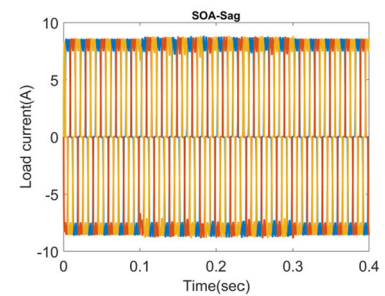
(a) Compensated load voltage waveform with FOPID –PI controller having CSO optimization at sag



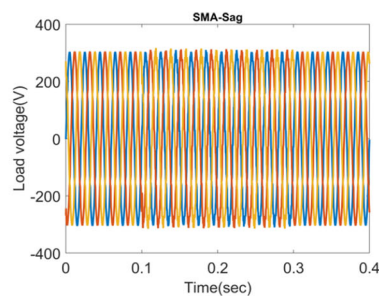
(b) Compensated current-voltage waveform with FOPID –PI controller having CSO optimization at sag



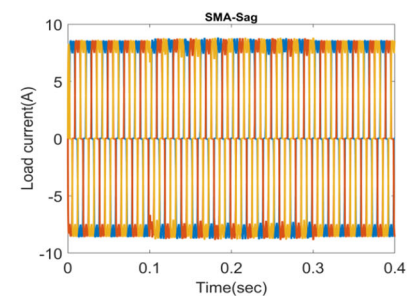
(c) Compensated load voltage waveform with FOPID –PI controller having SOA optimization at sag



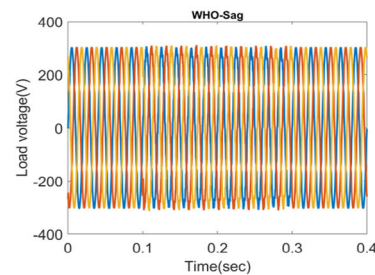
(d) Compensated load current waveform with FOPID –PI controller having SOA optimization at sag



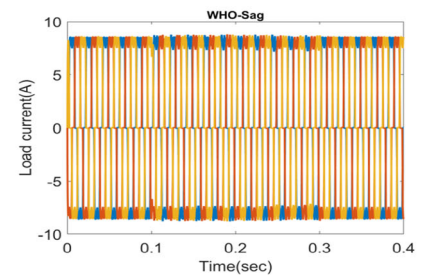
(e) Compensated load voltage waveform with FOPID –PI controller having SMA optimization at sag



(f) Compensated load current waveform with FOPID –PI controller having SMA optimization at sag

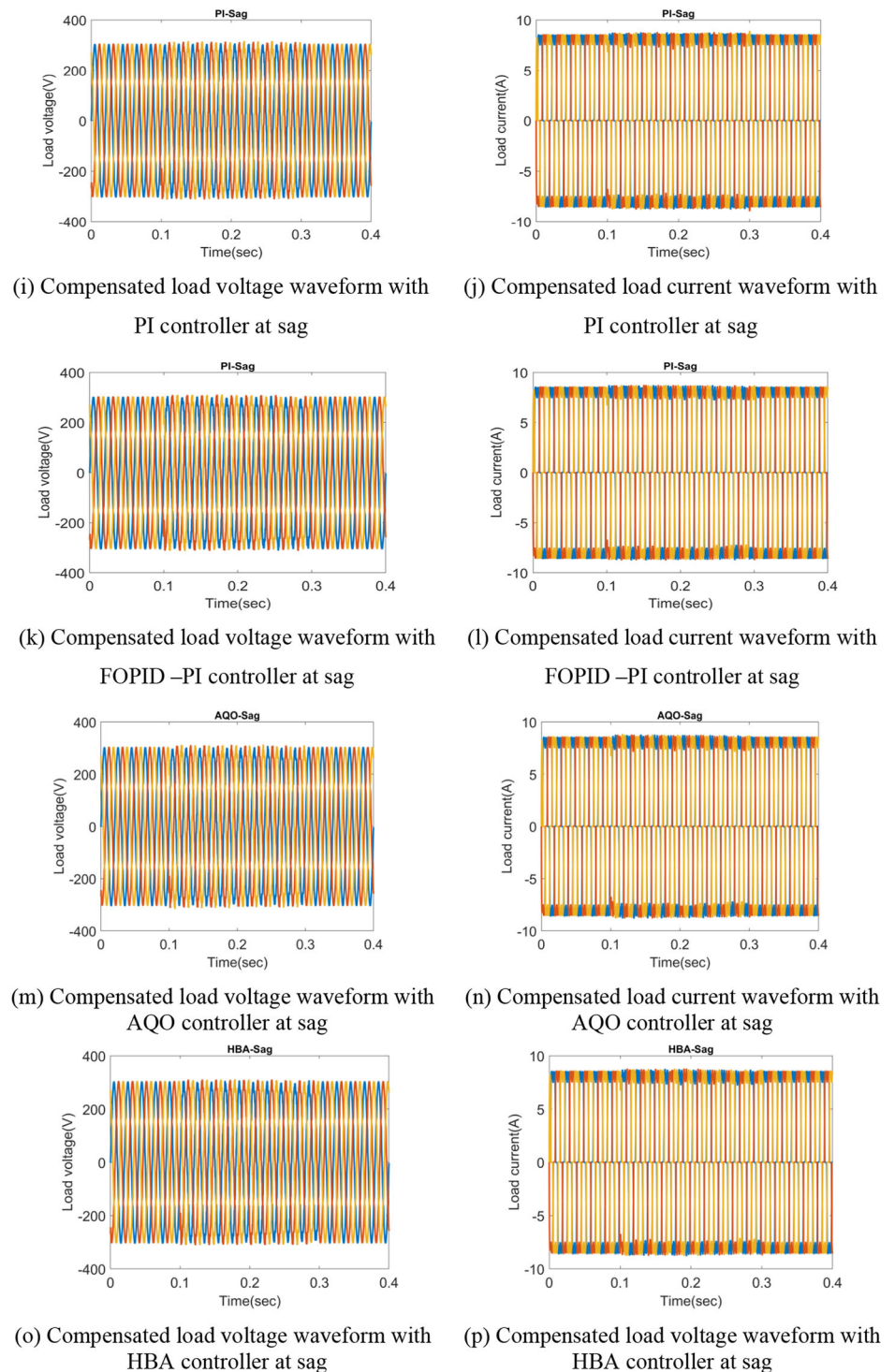


(g) Compensated load voltage waveform with FOPID –PI controller having WHO optimization at sag



(h) Compensated load current waveform with FOPID –PI controller having WHO optimization at sag

Fig. 7 continued



5 Optimal tuning of gain parameters using hybrid ASM-WHO algorithm

Recently, MAs have become more popular in many practical fields as they perform better and need less computational power and time than the predetermined optimization algorithms. MAs are often motivated by natural

observations of biological processes to develop better solutions to optimization issues. It is a global optimization approach with stronger resilience and application. Bio groupings in nature that have social behaviour and intellect to pursue a specific goal are frequently the source of inspiration. Despite their differences, all MAs have two steps in search optimization: exploration and exploitation

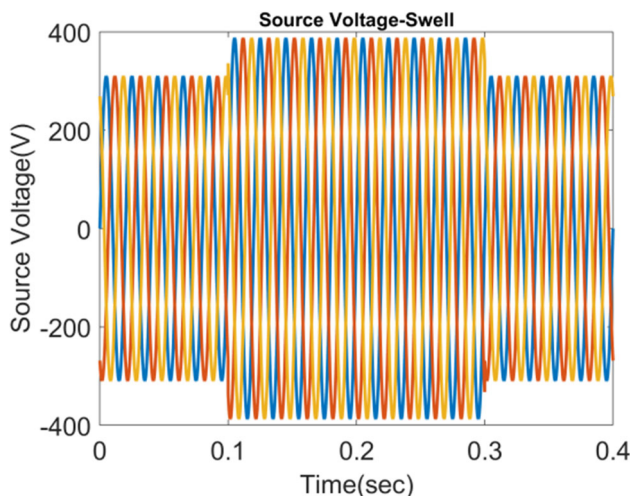


Fig. 8 Source voltage waveform without UPQC

(Lin and Gen 2009). The exploration phase entails probing the search area feasibly as broad, random, and worldwide. The algorithm’s ability to précised searching gained at the exploration phase is referred to as the exploitation phase. Thus, finding a good balance between the two phases that is efficient for all optimization tasks is quite difficult. This paper offers a more adaptable and efficient meta-heuristic algorithm by combining the aspects of the WHO with SMA. Here, the proposed method optimally tunes the gain parameters, such as k_p, k_i, k_d fractional orders (λ, μ) and weight parameters (w_1, w_2), thereby regulating the DC link voltage.

5.1 Slime mould algorithm

Slime mould is a unicellular organism that thrives in chilly, moist environments. With a special mathematical model that mimics the biological wave using adaptive weights, it has some novel features. It offers the best route for establishing a connection between food and highly effective exploration and exploitation. Plasmodium is the energetic movement stage of slime mould, which is a major nutritional stage, where the organic matter searches for food, traps, and produces enzymes to break it down. The extreme part of the cell forms a fan-shaped structure accompanied by an interlinked vein structure which permits a cytoplasmic move within (Li et al. 2020). With their distinct pattern and features, they may utilize many food sources simultaneously by developing interlinked veins. A propagation wave is produced by the bio-oscillator dependent on the calibre of the meal. When a vein hits a supply of high-quality food, it speeds up the cytoplasm flow to produce a thicker vein; conversely, if the food quality is relatively low, slime mould moves on to find a better food source. The slime constructs the perfect link to the food using this mix of positive and negative signals (Latty and Beekman 2015). Several actions of the slime mould stated above were mathematically represented below.

5.1.1 Food exploration

The stench of food simulates the slime mould to search for food. The fungus permits the extension of its exterior layer

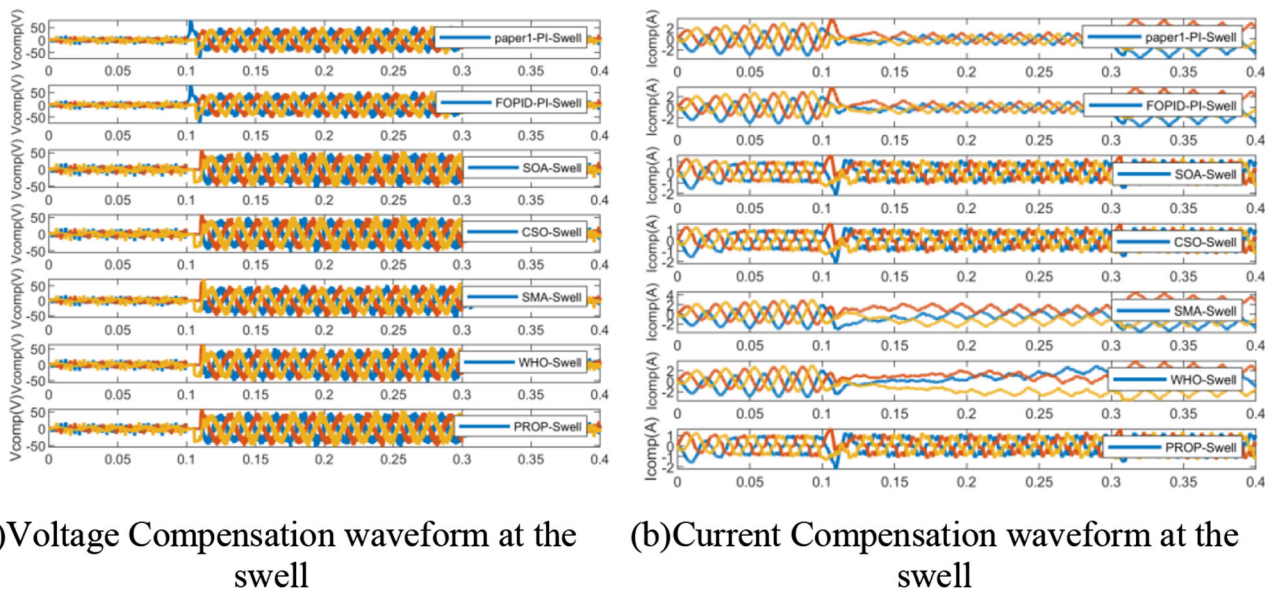
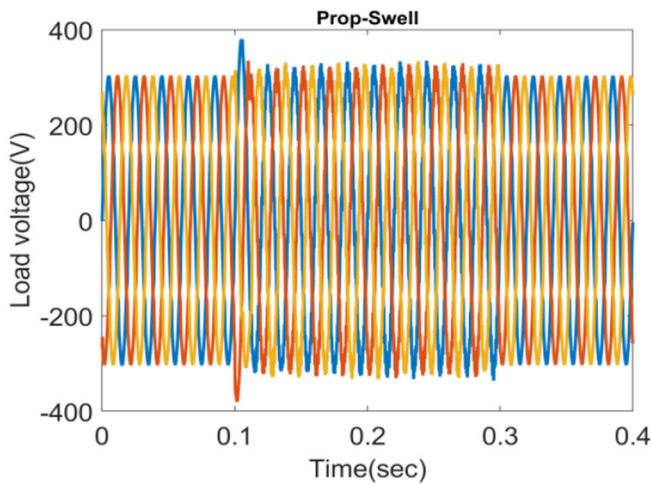
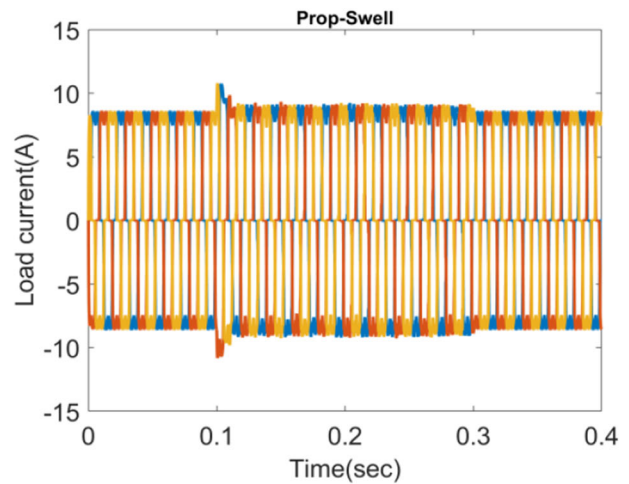


Fig. 9 Compensation waveforms of the suggested approach over the extant methods under Swell condition



(a) Compensated load voltage waveform with proposed optimized controller



(b) Compensated load current waveform with proposed optimized controller

Fig. 10 Case 1— Proposed approach under Swell condition, (a) Compensated Load voltage and (b) Compensated current waveform

in response to environmental smell variations. Depending on the amount of food present, the cytoplasmic flow in the enlarged vein rises to widen the vein and form a thick link. When food quality is poor or knowledge about food is lacking, a recession occurs in extension and attempts to discover alternative sources. The method of food approach is mathematically formulated as

$$Y_x = Y_b + v_b * (W_S * (Y_A - Y_B)), \quad s_r < l \tag{4}$$

$$Y_x = v_c * Y_x; \quad s_r \geq l \tag{5}$$

where v_c decreases from 0 to 1, x represent the iteration, Y_b the best place at the moment with the most stench, and Y_A, Y_B the two slime moulds that were chosen at random. The value represented by s_r is a random number between 0 and 1:

$$l = \tanh|F(i) - F_b| \tag{6}$$

where $i \in 1, 2 \dots n$, where $F(i)$ denotes the fitness of Y , while F_b stands for the best alliteration fitness. v_b is the parameter, which spans from $-a$ to a , in which

$$a = \operatorname{arctanh}\left(-\left[\frac{1}{\max_x}\right](x) + 1\right) \tag{7}$$

The slime mould search position can be optimized by changing the values of v_b and v_c . The condition simulates the food search pattern of slime mould.

5.1.2 Food wrapping

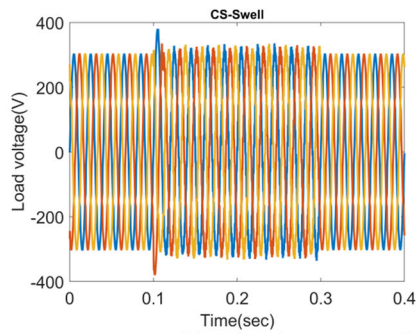
When the food availability is high, a strong bio-oscillator wave increases the flow of cytoplasm to initiate the slime mould contraction and make thicker the vein. The correlation of slime mould’s vein width contraction and the availability of food is updated using the following equation:

$$\overrightarrow{W_{S(i,j)}(\text{smellindex})} = \begin{cases} 1 + s_r * \log\left(\frac{F_b - F(i,j)}{F_b - F_w} + 1\right); & 1 \leq F(i) \leq \frac{1}{2}N_s \\ 1 - s_r * \log\left(\frac{F_b - F(i,j)}{F_B - F_w} + 1\right); & \frac{1}{2}N_s \leq F(i) \leq N_s \end{cases} \tag{8}$$

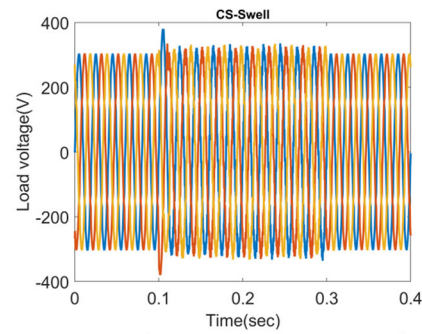
where, $\overrightarrow{W_{S(i,j)}(\text{smellindex})}$ represents the weight of slime mould, and the smell index denotes the sorted values of the sequence of fitness. F_w denotes the worst fitness, N_s denotes the population.

5.1.3 Food grabbing

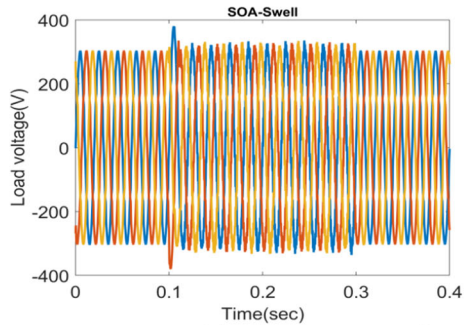
Based on the bio oscillation wave slime mould modifies the flow of cytoplasm through veins, which allows the slime mould to find a better food content. $\overrightarrow{W_{S(i,j)}(\text{smellindex})}$ mathematically replicates the oscillation frequency hence the slime mould may move fast towards the food as they locate enriched content of food and move slowly when is



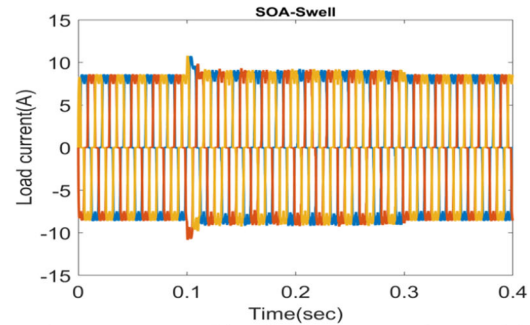
(a) Compensated load voltage waveform with FOPID –PI controller having CSO optimization at the swell



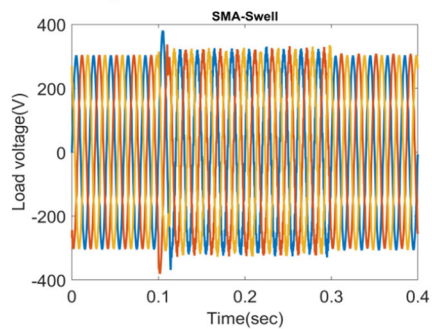
(b) Compensated current-voltage waveform with FOPID –PI controller having CSO optimization at the swell



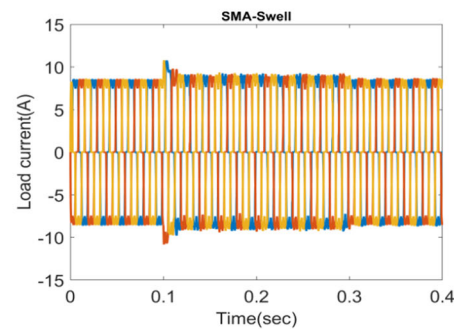
(c) Compensated load voltage waveform with FOPID –PI controller having SOA optimization at the swell



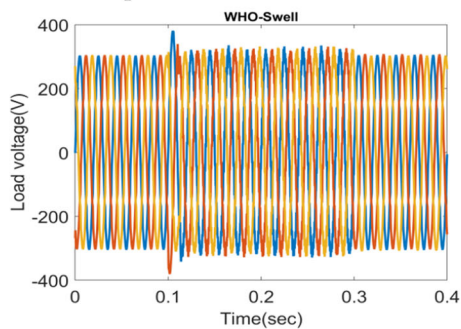
(d) Compensated load current waveform with FOPID –PI controller having SOA optimization at the swell



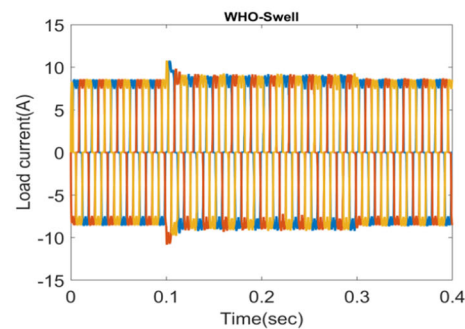
(e) Compensated load voltage waveform with FOPID –PI controller having SMA optimization at the swell



(f) Compensated load current waveform with FOPID –PI controller having SMA optimization at the swell



(g) Compensated load voltage waveform with FOPID –PI controller having WHO optimization at swell



(h) Compensated load current waveform with FOPID –PI controller having WHO optimization at swell

◀**Fig. 11** Comparison of Compensated Load voltage and current waveform of the suggested approach over the extant methods under Swell condition

low, enhancing the slime mould’s efficiency in selecting the best food source. As the slime mould finds the high-content food, the vein weight increases; while the vein weight decreases if the food content is low which causes search agents to explore other areas. The slime mould location updating is given by

$$Y_x = (U_b - L_b) * s_{rand} + L_b; \quad s_{rand} < m \tag{9}$$

where, U_b and L_b are the upper and lower boundaries of search respectively, s_{rand} generated randomly between 0 and 1, m is the probability of SMA to search for another food source preferable to the present.

5.2 Wildebeest herd optimization algorithm

The WHO algorithm is a new global search optimization algorithm developed based on the stimulus evolved by observing the individual and herd migration of wildebeests searching high-density grassland with the objective to minimum cost evaluation. Each movement and the corresponding mathematical modeling of the WHO algorithm are explained in the following steps (Amali and Dinakaran 2019). The dispersion of a herd of wildebeest in the field is depicted as a set of random points in the search region.

5.2.1 Local movement (Milling behavior)

The purblind wildebeest, which primarily relies on sniffing and hearing, can search for food only within a limited region (Ben-Shahar and Coe 1992). Let N_w be the fixed number of steps for each exploration. Each step of the wildebeest varies in length, and hence random exploration of a wildebeest X is defined as,

$$E = X + \eta uv \tag{10}$$

where η refers to constant, u refers to a uniform random number (0,1) multiplied by the random unit vector v . Furthermore, concerning the exploration E , a, N_w number of steps were taken to approach the newly identified best position. This movement is defined as

$$X = \alpha E^* + \beta(X - E^*) \tag{11}$$

5.2.2 Herd Instinct

With herd intuition, wildebeests approach the random individual far from the herd in the region of high grass density. The crowd in the herd and the poor vision of the wildebeest make the instinct less probable. The Wildebeest at X finding another random individual located X^h near high-density grass is defined as,

$$X = \alpha_1 X + \beta_1 X^h \tag{12}$$

5.2.3 Starvation avoidance

To escape famine, wildebeests migrate away from areas threatened with extinction (Amali and Dinakaran 2019). Wildebeest moves from the area with the least grass to find a better solution.

$$X^* = X + s_r(U_b - L_b)\hat{v} \tag{13}$$

where \hat{v} (random unit vector) and s_r ranges between [0, 1], U_b and L_b refers to the upper and lower boundary of search space, respectively.

5.2.4 Population pressure

The wildebeest are conscious of prevention from local clashes to move away and balance their shift from congested areas to high grass-density locations. (Thaker et al. 2010). The regional disputes due to the population pressure in high-density grasslands allow the strongest wildebeest to stand over and induce the relocation of losers far from high-density grasslands to the second-best solution.

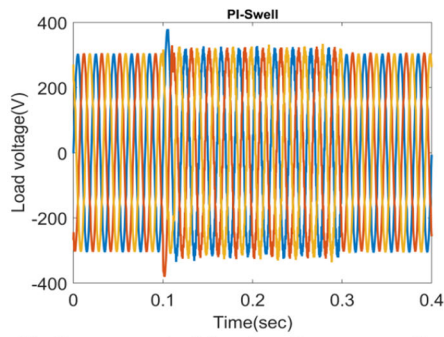
5.2.5 Herd social memory

Ultimately, the overall wildebeest in the herd maintains memories of previously known productive places with high grass density (Latty and Beekman 2015). Furthermore, it also inquiries about the previously identified excellent places and models as,

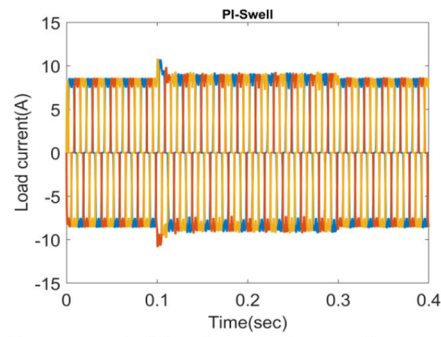
$$X = X^* + 0.1\hat{v} \tag{14}$$

In the proposed ASM-WHO algorithm, the slime mould position search is amplified by appending the wildebeest exploration for starvation avoidance and the best position search by social memory. Algorithm 1 contains the suggested ASM-WHO strategy’s pseudocode.

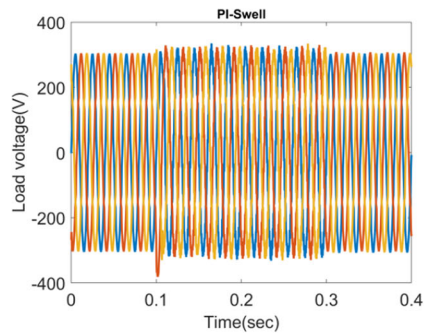
Algorithm 1:Proposed Slime Mould Algorithm –WHO model.



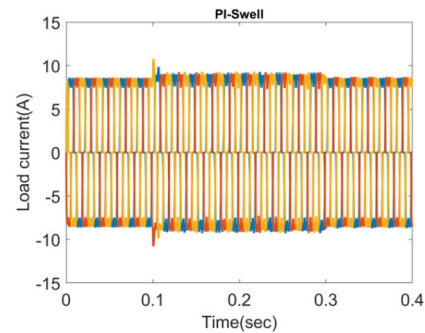
(i) Compensated load voltage waveform with PI controller at swell



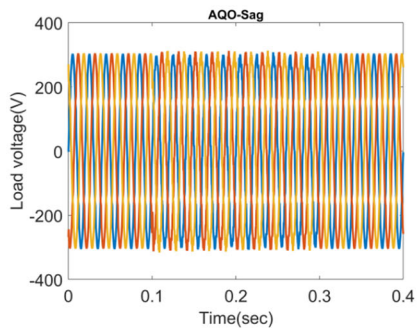
(j) Compensated load current waveform with PI controller at swell



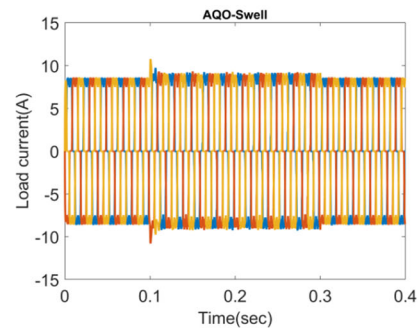
(k) Compensated load voltage waveform with FOPID-PI controller at swell



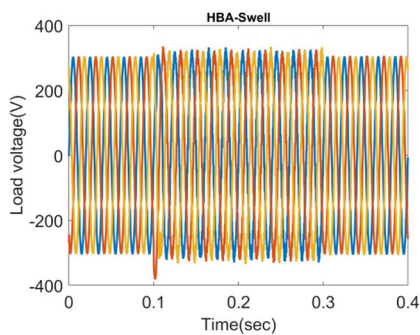
(l) Compensated load current waveform with FOPID-PI controller at swell



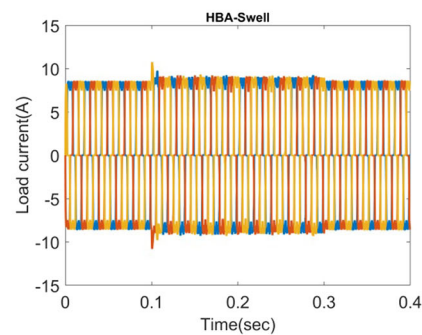
(m) Compensated load voltage waveform with AQO controller at swell



(n) Compensated load current waveform with AQO controller at swell



(o) Compensated load voltage waveform with HBA controller at swell



(p) Compensated load current waveform with HBA controller at swell

Fig. 11 continued

Step1: Initialization of parameters, $N_s, N_w, X, \max_itr, L_b, U_b$	
Step2: Initialize slime mould position $\vec{Y}_{(i,j)}$, Search space range L_b, U_b	
Step3: While $x \leq \max_itr$	
Step4: Update the best fitness F_b at the best position Y_b	
Calculate slime mould fitness $Y_{x(i,j)}$ $i \in 1, 2, \dots, N_s; j \in 1, 2, \dots, N_w$	
Calculate the Vein weight fitness using Eq. (8)	
Step5: Find the position of the best slime mould	
Update search agents	
For each search $i \in 1, 2, \dots, N_s$	
Update the location of slime mould using Eq.(9)	
For each exploration	
$s_r < l$	
Calculate Y_x, X^* using Eq.(4) and (13)	
$s_r \geq l$	
Calculate Y_x, X using Eq.(5) and (14)	
End for	
End for	
Step 6: Increment $x = x + 1$	
Step 7: End While	
Step 8: Return the Best fitness F_b	

6 Results and discussion

6.1 Experimental setup

By running the proposed model through a MATLAB simulation, the system performance is scaled out. The study took into account the supply voltage, load current,

and voltage concerning time when it was done under voltage sag and swell (0–0.4 s). The results of the proposed methodology which includes FOPID–PI controller with ASM-WHO optimization compared to the system model with PI controller, FOPID–PI collateral controller without optimization, and optimization algorithms such as CSO, SOA, SMA, WHO, Aquila Optimization algorithm (AO) (Abou El-Ela et al. 2022), and Honey Badger algorithm

Table 2 Stability Analysis for Proposed Work over Conventional Models

Measures	PI	FOPID-PI	SOA	CSO	SMA	WHO	AQO	HBA	Proposed Method
Rise Time	7191.6	7267.7	7193.5	7193.5	7193.5	7271.1	7276.6	7274	7282.6
Settling Min	7909.6	7926.3	7910.1	7910.1	7910.1	7927.7	7925.5	7924.9	7927.1
Settling Time	170.6	149.9	170.8	170.8	170.8	149.4	149.3	148.7	147.3
Settling Max	189.5	166.5	189.8	189.8	189.8	166	165.9	165.2	163.6
Overshoot	0	0	0	0	0	0	0	0	0
Undershoot	0	0	0	0	0	0	0	0	0
Peak	189.5	166.5	189.76	189.8	189.8	166	165.9	165.2	163.6
Peak time	8001	8001	8001	8001	8001	8001	8001	8001	8001

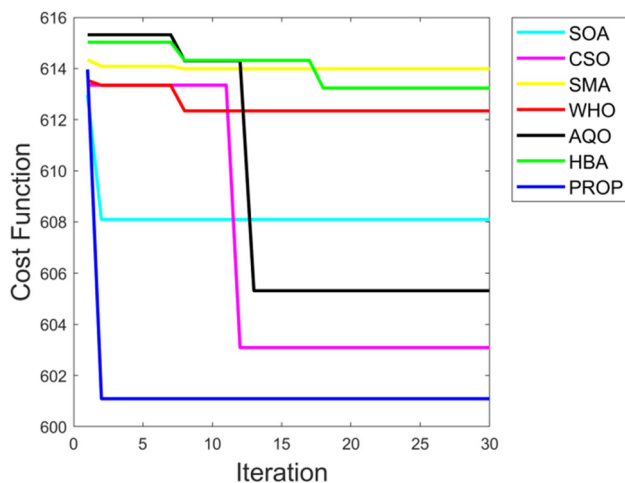


Fig. 12 Fitness evaluation for various methods compared

(HBA) (Khadanga et al. 2022). Table 1 depicts the algorithm parameters. Moreover, parameters such as “Rise time, Settling time, Settling minimum, Settling maximum, Overshoot, Peak and Peak time” are considered to verify the proposed model performance, which is discussed as follows:

Rise time: It is defined as the time required by the response to reach from zero value to a hundred percent value of the final value.

Settling time: The amount of time the response needs to take to attain and fall within the prescribed range of between (2% and 5%) of its ultimate value is known as the settling time.

Settling minimum: The settling minimum is the amount of time that is necessary for settling.

Settling maximum: Settling minimal is the amount of time that can be settled in.

Overshoot: This term refers to the response’s greatest positive deviance from the desired value.

Undershoot: When a transition is made from a higher to a lower value, undershoot occurs, because the initial value is lower than the final value.

Peak time: The period needed for the response to the peak value is referred to as peak time.

Case (i): Under Sag Condition

Initially, voltage sag arises at 0.1–0.3 s in the source voltage without UPQC. Figure 4 depicts the source voltage with sag.

Now the UPQC is triggered to inject a series of compensated voltage and shunt compensated current. Better compensation is provided by the UPQC when the controller is optimised. Figure 5 displays the compensation current and voltage. Figure 6 displays the sag freeloading voltage and current with UPQC.

Fig. 13 THD analysis for sag (A) PI (b) FOPID–PI (c) FOPID –PI with CSO (d) FOPID–PI with SOA (e) FOPID–PI with SMA (f) FOPID–PI with WHO (g) FOPID–PI with AQP (h) FOPID –PI with HBA (i) Proposed FOPID–PI controller with ASM –WHO

The resulting improved response signals with the proposed system are compared to the system model with PI controller, FOPID –PI collateral controller without optimization, and with optimization algorithms such as CSO, SOA, SMA, and WHO as deployed in Fig. 7. With improved compensation, the suggested model with the collateral controller is considered the best compensator, which can provide sinusoidal load voltage and current ideal with rated waveforms.

Case (ii): Under Swell Condition

Initially voltage swell arises at 0.1 to 0.3 s in the voltage from the grid without UPQC. Figure 8 displays the source voltage with swell.

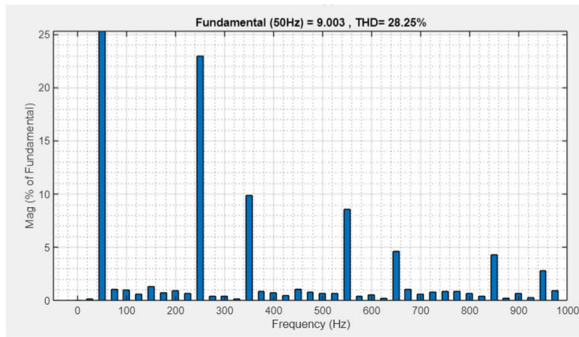
Now the UPQC is triggered to inject a series of compensated voltage and shunt compensated current. Better compensation is provided by the UPQC when the controller is optimised. Figure 9 displays the compensation current and voltage. Figure 10 displays the proposed UPQC’s distortion-free load voltage and current.

The resulting improved waveforms of the proposed method are compared to the system model with PI controller, FOPID –PI collateral controller without optimization, and with optimization algorithms such as CSO, SOA, SMA, and WHO as shown in Fig. 11. With improved compensation, the proposed model with a collateral controller is considered the best compensator which can provide sinusoidal load voltage and current ideal with rated waveforms.

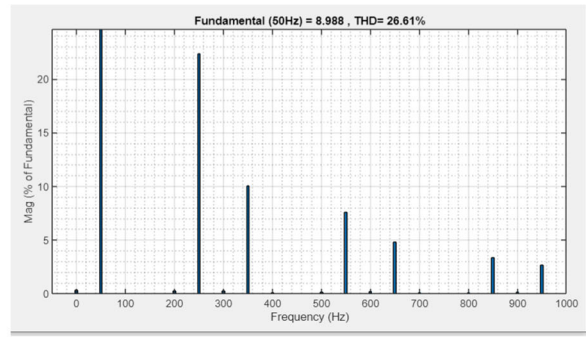
6.2 Stability analysis

The proposed optimal FOPID–PI collateral controller with ASM–WHO optimization’s steady-state response is contrasted with that of traditional approaches. In Table 2, responses were tallied according to such criteria as “rising time, settling time, settling minimum, settling maximum, overshoot undershoot, peak and peak time.” The proposed model is preferable since it requires less time to settle when compared to the standard approaches, according to the indicated fitness evaluation in Fig. 12. In addition, the convergence happens more quickly than with traditional approaches and requires less iteration for relatively inexpensive functions.

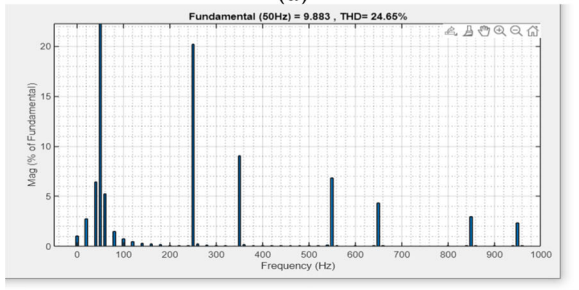
The settling time for the FOPID–PI controller with either SOA or CSO or SMA optimization takes 170.81 and 149.42 s with WHO optimization seconds. The settling time for the PI controller is 170.57 s. While the settling



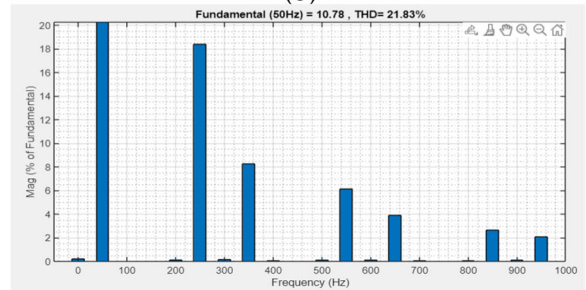
(a)



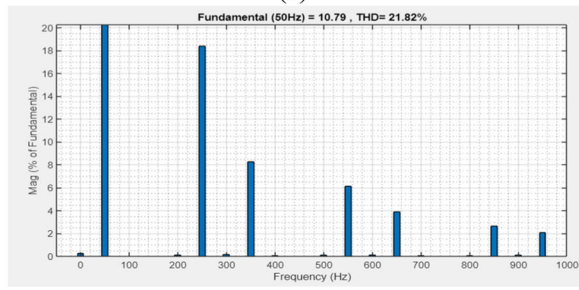
(b)



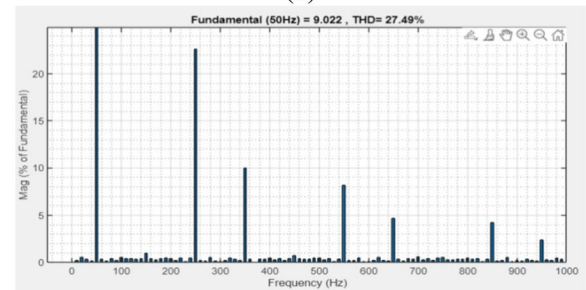
(c)



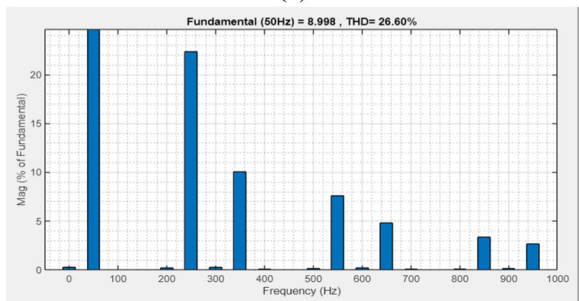
(d)



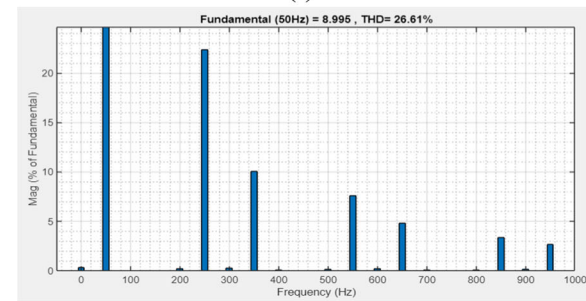
(e)



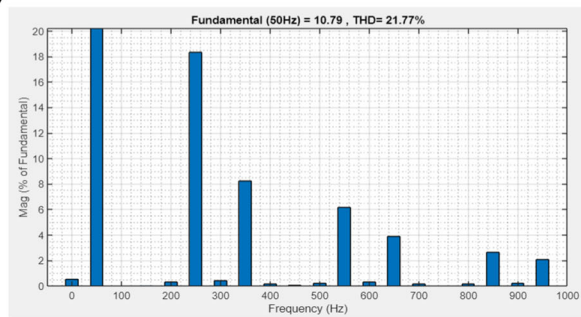
(f)



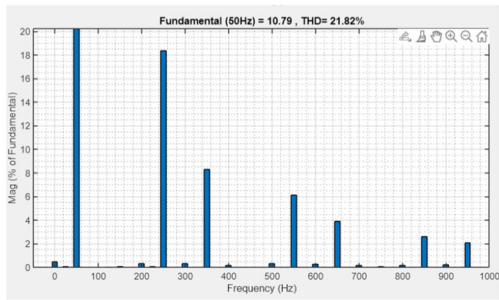
(g)



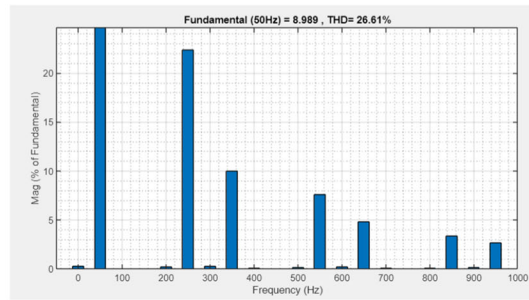
(h)



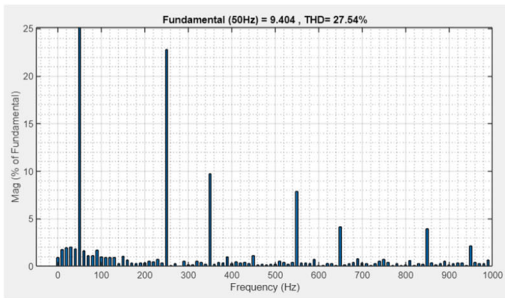
(i)



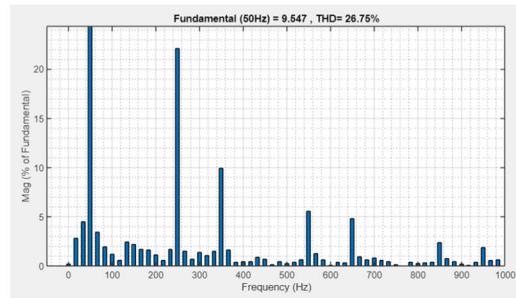
(a)



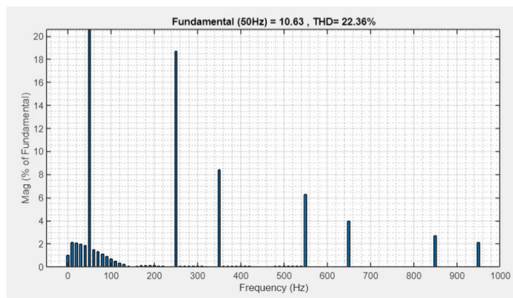
(b)



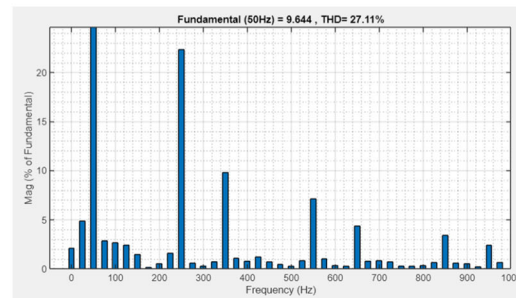
(c)



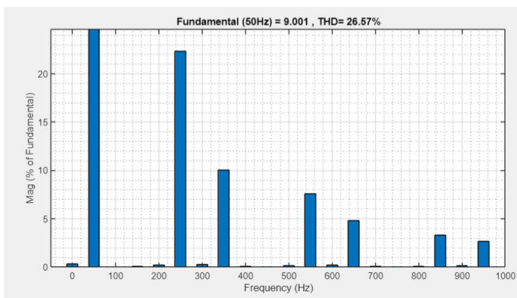
(d)



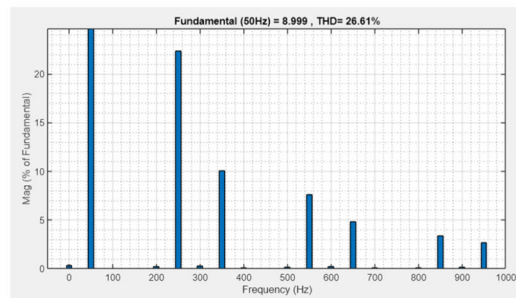
(e)



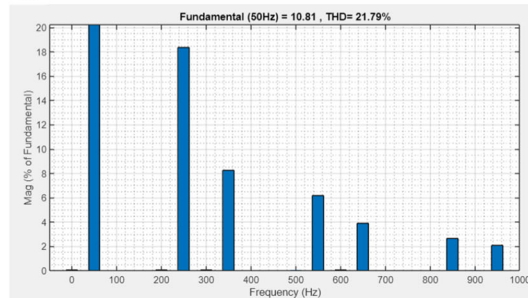
(f)



(g)



(h)



(i)

◀**Fig. 14** THD analysis for swell (a) PI (b) FOPID–PI (c) FOPID–PI with CSO (d) FOPID–PI with SOA (e) FOPID–PI with SMA (f) FOPID–PI with WHO (g) FOPID–PI with AO (h) FOPID–PI with HBA (i) Proposed FOPID–PI controller with ASM–WHO

time for the proposed FOPID–PI controller with ASM–WHO is 147.27 s, which is 1.7% better than the settling time of the controller without optimization, 13.78% better than the proposed collateral controller method with either SOA or CSO, or SMA optimization and 1.338% and 13.66% better than the method with WHO optimization and with PI controller, respectively.

Consequently, the enhanced results are tabulated below show that the proposed strategy is effective.

6.3 THD Analysis

Figures 13 and 14 depict the THD value of controllers, existing optimization and the proposed method. The FOPID–PI controller with ASM–WHO at sag has a lower percentage of harmonics of 21.77%, when compared to the existing controllers and existing models. Moreover the FOPID–PI controller with ASM–WHO at swell has a lower percentage of harmonics of 21.79%, PI controller, FOPID–PI collateral controller without optimization, and optimization algorithms, such as CSO, SOA, SMA, WHO, AQO and HBA. This portrays the effectiveness of the proposed model in proper harmonic reduction.

7 Conclusion

The effectiveness of a suggested optimal parameterized FOPID controller for three-phase UPQC coupled with hybrid RES, such as a PV-Wind-BESS system, was investigated in this work. The DC link in the shunt APF compensator was required to be controlled at the correct level using a reliable FOPID–PI control technique. Therefore, an Amplified Slime Mold with Wildebeest Herd Optimization (ASM–WHO) Algorithm is used to optimise the parameters of the collateral FOPID–PI controller to fine-tune the gain. The results of the analysis show that the suggested technique outperforms SOA, CSO, SMA, and WHO procedures in terms of sag and swell in the load current and load voltage, increasing the efficiency of the power system. The UPQC-integrated distribution system with ASM–WHO optimised FOPID–PI controller is approximately 13.78% better than the suggested controller with conventional algorithms and other traditional approaches, according to the stability study for the aforementioned methodologies. The future goal of this research is to improve the model's efficiency by modifying the

parameters with the use of modern hybrid optimization methods.

Funding This research did not receive any specific funding.

Data availability Data sharing is not applicable to this article as no new data were created or analyzed in this study.

Declarations

Conflict of interest The authors declare no conflict of interest.

Informed consent Not Applicable.

Ethical approval The conducted research is not related to either human or animal use.

References

- Abou El-Ela AA, El-Shehmy RA, Shaheen AM, Shalaby AS (2022) Aquila optimization algorithm for wind energy potential assessment relying on Weibull parameters estimation. *Wind* 2(4):617–635
- Alam SJ, Arya SR (2020) Observer-based control for UPQC-S with optimized gains of PI controller. *Int Trans Electr Energy Syst* 30(7): e47233.
- Amali D, Dinakaran M (2019) Wildebeest herd optimization: a new global optimization algorithm inspired by wildebeest herding behaviour. *J Intell Fuzzy Syst* 37(6):8063–8076
- Ben-Shahar R, Coe MJ (1992) The relationships between soil factors, grass nutrients and the foraging behaviour of wildebeest and zebra. *Oecologia* 90(3):422–428
- Carrasco JM, Franquelo LG, Bialasiewicz JT, Galván E, PortilloGuisado RC, Prats MM, León JI, Moreno-Alfonso N (2006) Power-electronic systems for the grid integration of renewable energy sources A survey. *IEEE Trans Industr Electron* 4:1002–1016
- D'Angelo G, Ficco M, Robustelli A An association rules-based approach for anomaly detection on CAN-bus, In: International conference on computational science and its applications, pp. 174–190. Cham: Springer Nature Switzerland, 2023
- Devassy S, Singh B (2017) Design and performance analysis of three-phase solar PV integrated UPQC. *IEEE Trans Ind Appl* 54(1):73–81
- Gianni D'Angelo, Eslam Farsimadan, Massimo Ficco, Francesco Palmieri, Antonio Robustelli, Privacy-preserving malware detection in Android-based IoT devices through federated Markov chains, *Future Generation Computer Systems*, <https://doi.org/10.1016/j.future.2023.05.021>.
- Gowrishankar A, Ramasamy M (2020) SPV-based UPQC with modified power angle control scheme for the enhancement of power quality. *J Circ Syst Comput* 29(04):2050064
- Goud BS, Loveswara Rao B (2021) Power quality enhancement in grid-connected PV/wind/battery using UPQC: atom search optimization. *J Electr Eng Technol* 16(2): 821–835.
- Javadi A, Hamadi A, Woodward L, Al-Haddad K (2016) Experimental investigation on a hybrid series active power compensator to improve the power quality of typical households. *IEEE Trans Industr Electron* 63(8):4849–4859

- Jin T, Chen Y, Guo J, Wang M, Mohamed MA (2020) An effective compensation control strategy for power quality enhancement of unified power quality conditioner. *Energy Rep* 6:2167–2179
- Jumani TA, Mustafa MW, Hussain Z, Md Rasid M, Salman Saeed M, Memon MM, Khan I, Nisar KS (2020) Jaya optimization algorithm for transient response and stability enhancement of a fractional-order PID based automatic voltage regulator system. *Alexandria Eng J* 59(4): 2429–2440.
- Kumar S, Malleshham G (2020) Performance of three phase AI controller based UPQC to enhance power quality of hybrid RES. *Microsystem Technologies* 26(8): 2673–2682.
- Kumar CP, Pragaspathy S, Karthikeyan V, Durga Prakash KNS Power quality improvement for a hybrid renewable farm using UPQC. In: 2021 International conference on artificial intelligence and smart systems (ICAIS), pp. 1483–1488. IEEE, 2021.
- Khadkikar V (2011) Enhancing electric power quality using UPQC: A comprehensive overview. *IEEE Trans Power Electron* 27(5):2284–2297
- Khadanga RK, Nayak SR, Panda S, Das D, Prusty BR, Sahu PR (2022) A novel optimal robust design method for frequency regulation of three-area hybrid power system utilizing honey badger algorithm. *Int Trans Electr Energy Syst* 2022.
- Latty T, Beekman M (2015) Slime moulds use heuristics based on within-patch experience to decide when to leave. *J Exp Biol* 218(8):1175–1179
- Latha YK, Saibabu C, Obulesu YP (2011) Unified Power Quality Conditioner for voltage sag and harmonic mitigation of nonlinear loads. *Int J Power Electron Drive Syst* 1(1):65–74
- Lei T, Riaz S, Zanib N, Batool M, Pan F, Zhang S Performance Analysis of grid-connected distributed generation system integrating a hybrid wind-PV farm using UPQC. *Complexity* 2022 (2022).
- Lin L, Gen M (2009) Auto-tuning strategy for evolutionary algorithms: balancing between exploration and exploitation. *Soft Comput* 13(2):157–168
- Li S, Chen H, Wang M, Asghar Heidari A, Mirjalili S Slime mould algorithm: A new method for stochastic optimization. *Future Generation Computer Systems* 111 (2020): 300–323.
- Mansor MA, Hasan K, Othman MM, Mohammad Noor SZB, Musirin I (2020) Construction and performance investigation of three-phase solar PV and battery energy storage system integrated UPQC. *IEEE Access* 8: 103511–103538.
- Mahdi DI, Gorel G (2022) Design and control of three-phase power system with wind power using a unified power quality conditioner. *Energies* 15(19):7074
- Nanthagopal DrSC (2020) Power Quality Improvement Using Three-Phase Solar PV Integrated UPQC. *Int J Modern Trends Sci Technol* ISSN: 2455–3778 :: 06(07)
- Naidu RPK, Meikandasivam S (2020) Power quality enhancement in a grid-connected hybrid system with coordinated PQ theory & fractional order PID controller in DPFC. *Sustain Energy Grids Netw* 21: 100317.
- Nehrir MH, Wang C, Strunz K, Aki H, Ramakumar R, Bing J, Miao Z, Salameh Z (2011) A review of hybrid renewable/alternative energy systems for electric power generation: configurations, control, and applications. *IEEE Trans Sustain Energy* 2(4):392–403. <https://doi.org/10.1109/TSTE.2011.2157540>
- O'Dwyer A (2000) A summary of PI and PID controller tuning rules for processes with time delay. Part 1: PI controller tuning rules. *IFAC Proceedings Volumes* 33(4):159–164
- Qazi A, Hussain F, Rahim NA, Hardaker G, Alghazzawi D, Shaban K, Haruna K Towards sustainable energy: a systematic review of renewable energy sources, technologies, and public opinions. *IEEE Access* 2019, 7: 63837–63851. [CrossRef]
- Reddy CB, Srikanth G Aymen F, Srinivasa Rao G, Bortoni EC (2021) Power Quality improvement in HRES grid connected system with FOPID based atom search optimization technique. *Energies* 14(18): 5812.
- Sadigh AK, Smedley KM (2012) Review of voltage compensation methods in dynamic voltage restorer (DVR). In: 2012 IEEE power and energy society general meeting, pp. 1–8. IEEE
- Samal S, Hota PK (2017) Power Quality Improvement by Solar Photo-voltaic/Wind Energy Integrated System Using Unified Power Quality Conditioner. In: *Int J Power Electron Drive Syst (IJPEDS)* 8(3): 1416–1426, ISSN: 2088–8694, <https://doi.org/10.11591/ijpeds.v8i3>.
- Singh B, Jain C, Goel S, Chandra A, Al-Haddad K (2016) A multifunctional grid-tied solar energy conversion system with ANF-based control approach. *IEEE Trans Ind Appl* 52(5):3663–3672
- Sivakumar M, Kannan P, Chenthur Pandian S (2019) Mitigation of PQ issues using an enhanced UPQC-based ANN approach. *J Circ Syst Comput* 28(03):1950046
- Singh B, Chandra A, Al-Haddad K Power quality: problems and mitigation techniques. John Wiley & Sons
- Subudhi B, Pradhan R (2012) A comparative study on maximum power point tracking techniques for photovoltaic power systems. *IEEE Trans Sustain Energy* 4(1):89–98
- Thaker M, Vanak AT, Owen CR, Ogden MB, Slotow R (2010) Group dynamics of zebra and wildebeest in a woodland savanna: effects of predation risk and habitat density. *PLoS ONE* 5(9):e12758
- Thangella R, Yarlagadda SR, Sanam J (2023) Optimal power quality improvement in a hybrid fuzzy-sliding mode MPPT control-based solar PV and BESS with UPQC, *Int J of Dyn Control* 11(4): 1823–1843.

Publisher's Note Springer Nature remains neutral with regard to jurisdictional claims in published maps and institutional affiliations.

Springer Nature or its licensor (e.g. a society or other partner) holds exclusive rights to this article under a publishing agreement with the author(s) or other rightsholder(s); author self-archiving of the accepted manuscript version of this article is solely governed by the terms of such publishing agreement and applicable law.